Biosensors and Bioelectronics 91 (2017) 82–88

Contents lists available at ScienceDirect

Biosensors and Bioelectronics

journal homepage: www.elsevier.com/locate/bios

A green and facile approach for synthesizing imine to develop optical biosensor for wide range detection of bilirubin in human biofluids

Sundaram Ellairaja[a], Kathiravan Shenbagavalli[a], Sarkaraisamy Ponmariappan[b], Vairathevar Sivasamy Vasantha[a,*]

[a] Department of Natural Products Chemistry, School of Chemistry, Madurai Kamaraj University, Madurai 625021, Tamil Nadu, India
[b] Biotechnology Division, Defence Research Development & Establishment, Jhansi Road, Gwalior 474002, Madhya Pradesh, India

ARTICLE INFO

Keywords:
Bilirubin, 2,2′-((1E,1′E)-((6-bromopyridine-2,3-diyl) bis(azanylylidene)) bis(methanylylidene)) diphenol
Fluorimetry biosensor
Colorimetric biosensor
Lifetime study
Competitive study
Sonochemical synthesis
Imine molecule

ABSTRACT

Bilirubin, a key biomarker for the jaundice and its clinical diagnosis needs a better analytical tool. A novel and simple fluorescent platform based on (2,2′-((1E,1′E)-((6-bromopyridine-2,3-diyl) bis(azanylylidene)) bis(-methanylylidene diphenol) (BAMD) was designed. BAMD showed a remarkable fluorescent intensity with a very good quantum yield of 0.85 and lifetime of 870 ps. Hence, it was applied for the determination of bilirubin using both colorimetric and fluorimetric techniques in physiological and basic pH. Under optimized experimental conditions, the probe detects bilirubin selectively in the presence of other interfering biomolecules and metal ions. The linear range of detection is 1 pM–500 μM at pH=7.4 and LOD is 2.8 and 3.3 pM at pH=7.4 and 9.0, respectively, which were reported so far. The probe detects the bilirubin through FRET mechanism. The practical application of the probe was successfully tested in the human blood and urine samples. Based on all above advantages, this simple idea can be applied to design a simple clinical diagnostic tool for jaundice.

1. Introduction

During the enzymatic reaction of heme oxygenase enzyme on heme system, the precursor biliverdin is produced and then it is further processed by biliverdin reductase to covert the final bilirubin. Generally bilirubin is classified into three major categories as direct, (conjugate with glucuronic acid), indirect (not conjugated with glucuronic acid) and total bilirubin (direct and indirect bilirubin) (Cheifetz et al., 2010). Once it is conjugated in the liver, bilirubin is excreted into the bile and transported through the gut with food and further broken down, contributing to the color of stool (Thor and Ruud, 2010). It is a real threat full factor among humans to diagnosis the jaundice because of its acute fatal. The normal level of bilirubin in human blood is < 25 μmol (< 1.2 mg/dL) and in jaundice condition the level is increased to > 50 μmol/L (> 2.5 mg), which finally leads liver disorder (Silbernagl and Despopoulos, 2009). Considering these serious health issues, an accurate detection of bilirubin concentration in human serum is clinically becoming more important. Earlier, some methods include enzymatic assay using bilirubin oxidase (Morimoto et al., 2000) and vanadate oxidation assays (Ameri et al., 2011) had been used to detect the bilirubin in human serum. Currently, most available clinical methods are measuring the conjugated (direct) and total bilirubin using a classic spectrophotometric method based on the endpoint diazo reactions. However, it has some drawbacks like less stability, degradation, decoloration etc., (Rand and di Pasqua, 1962).

After a keen review of literatures reported, it is clearly understood that only a very few biosensors have been reported for the detection of bilirubin so far. Various electrochemical biosensors with different biocompatible platforms containing nanomaterials and bilirubin oxidase (BOx) have been used for the detection of bilirubin (Kannan et al., 2011; Feng et al., 2013; Batra et al., 2013;). For example, by utilizing BOx enzyme on gold micro electrode, a simple and selective sensor has also been reported (Jagriti et al., 2015). Recently, a non-enzymatic bilirubin (BR) sensor has also been developed based on spin coated reduced graphene oxide (RGO)–poly styrene sulfonate (PSS) composite film on a glassy carbon electrode (Balamurugan and Sheela, 2015).

Fluorimetric is also a powerful analytical tool to detect various toxic metal ions and biomolecules owing to its operational simplicity and very high sensitivity with a wide analyte concentration range. (Komatsu et al., 2007; Nolan and Lippard, 2007; Yoon et al., 2005; Kwon et al., 2005; Wang et al., 2006; De Silva et al., 1997; Miao et al., 2016; Xiao et al., 2013). A fluorimetric biosensor based on Au nanoparticles-conjugated HSA protein was reported for the sensing of bilirubin in human serum (Santhosh et al., 2014). In this study, the quenching emission profile of human serum albumin (HSA) stabilized gold nanoclusters was observed upon interaction with bilirubin. But for

* Corresponding author.
E-mail address: vasantham999@yahoo.co.in (V.S. Vasantha).

http://dx.doi.org/10.1016/j.bios.2016.12.026
Received 27 September 2016; Received in revised form 9 December 2016; Accepted 10 December 2016
Available online 11 December 2016
0956-5663/

the first time, another research group has reported fluorescent biosensor using water soluble polyfluorene polymer for the bilirubin detection with the limit of detection in nanomolar range (150 nM) in human blood plasma (Senthilkumar and Asha, 2015).

In general, imine based fluorescent molecules show a very good response towards various metal ions (Soojin et al., 2012). But, biomolecule concern, only a very few reports are available especially for amino acids since from the last decades (Ellen and Timothy, 2003). Further, no imine based fluorescent sensor is reported so far for most important biomolecules like dopamine, ascorbic acid, creatinine and bilirubin. Generally, most of our disease causing pathogens and biomolecules could have a tendency to bind with hydroxyl groups of glucose unit present in our body (Cuihua et al., 2006). Generally, these disease relating pathogens or biomolecules contains functional groups like amide, primary or secondary amines etc. and they are having a tendency to form hydrogen bonding with the hydroxyl group which is present in the carbohydrates. Similar type of intermolecular hydrogen bonding is also possible between organic molecules containing –OH and amines groups (Ravi et al., 2015; Oscar et al., 2011; Leo and Kline, 1950; Ambler, 1929; Reem and Moustafa, 2010; Gary and Ronald, 1980; Atsushi et al., 1996). We have synthesized a simple new imine 2,2′-((1E,1′E)-((6-bromopyridine-2,3-diyl)Bis (azanylylidene)) bis(-methanylylidene)) diphenol based fluorescent molecule and applied for the determination of bilirubin since it has hytroxy groups. The structure and photophysical studies of the synthesized molecule were done using various analytical techniques. Compare to the previous reports, our synthetic scheme is very simple, cost effective, less time consuming (10 min) and also followed a green synthetic route. We have designed a fluorescent biosensor based on the above BAMD moiety for the determination of direct bilirubin at two different pHs (7.4 and 9.0) and it was found that the biosensor was sensitive and selective towards bilirubin in the presence of other interfering biomolecules and metal ions. The detection limit and linear range of the biosensor towards bilirubin is very good comparing to earlier reports.

2. Materials and methods

2,3 - Diamino-5-Bromo Pyridine, Salicyaldehyde, Glacial Acetic acid, HPLC grade ethanol, Bilirubin, Uric Acid, Urea, Creatinine, Creatine, L-Dopamine, Ascorbic Acid, D-Glucose, and various acetate salts of metal ions (Zn^{2+}, Cd^{2+} Ca^{2+}, Ag^{+}, Na^{+}, K^{+}, Fe^{2+} Fe^{3+}, Co^{2+}, and Cu^{2+}) were purchased from Sigma Aldrich and used as such. The human serum was isolated from the blood of the students at Department of Chemistry, School of Biotechnology, Madurai Kamaraj University, Madurai.

^{1}H and ^{13}C NMR analysis was done using $CDCl_3$ and DMSO-d_6 as solvents containing a trace quantity of tetramethylsilane (TMS) as internal standard using Bruker- 300 MHz spectrometer and chemical shifts were reported in ppm at 25 °C. Mass spectra and UV spectra were recorded. Using ESI ionization in MS-LCMS mass spectrometer and SHIMADZU single beam UV–vis spectrophotometer, respectively. Fluorescent measurements were done using Cary Eclipse spectrophotometer having a 450 W xenon lamp. Fluorescence lifetime decays were counted using FLS 980 setup from EDINBURGH INSTRUMENTS U.K, with a λmax=435 nm) having a full width at half-maximum of 89 ps as a sample excitation source. The 5 nm and 2.5 nm were maintained as excitation and emission slit widths, respectively, throughout the experiments.

3. Synthesis and characterization of 2,2′-((1E,1′E)-((6-bromopyridine-2,3-diyl) bis(azanylylidene)) bis(methanylylidene)) diphenol (BAMD)

Usually irradiation with high intensity sound or ultrasound, acoustic cavitations occurs and results the implosive collapse of bubbles. These bubbles have temperature around 5000 K and pressure of roughly 1000 atm that are actually not achieved by normal or conventional synthetic method which requires more reaction time. So herein, we have used sonochemical method for the synthesis of BAMD. Briefly, 2,3 –diamino-5 bromo pyridine (1.0 g, 5 mmol, 1 equiv.)] was dissolved in 10 mL of absolute ethanol (solution) and mixed with solution (II) which was prepared by dissolving salicyaldehyde (1.3 g, 10 mmol, 2 equiv) in 5 mL of ethanol solution and then 0.5 mL of glacial acetic acid was added into the mixture. The mixture becomes slightly brown color and it was sonicated for 10 min and a dark-yellow colored solution was obtained. The resulting solution was allowed to cool at room temperature and a yellow product (III) was formed (Fig. S1.). The crude product was washed twice with ethanol and diethyl ether and dried over $MgSO_4$ under vacuum. The completion of product formation was confirmed by Thin Layer Chromatography (appearance of single spot). The yield was found to be 1.97 g (98%). We have performed the same reaction under normal reflux condition for 3 h and obtained only 92% yield. So, to the best of our knowledge, this method is first fast method for the synthesis of imine. Meanwhile, we have also compared the yield of the molecules with imine molecules prepared by sonochemical method reported previously. Only 90% yield was obtained at 15 min previously. (Christabel and Cheng-Wei, 2009; Thomas et al., 2009; Anjali et al., 2013; Cintas and Luche, 1999; Mason, 1997; Cravotto and Cintas, 2006). In order to confirm the reliability of the method, the reaction was repeated for 3 times and obtained the same results.

The NMR data for the synthesized imine are given below. ^{1}H NMR (300 MHz, $CDCl_3$, 298): δ=13.20 (s, 1 2 H), 12.57 (s, 2 H), 9.45 (s, 1 H), 8.61 (s, 1 H), 7.68 (d, 1 H), 7.50 (m, 7 H) ppm.^{13}C NMR (300 MHz, $CDCl_3$, 298 K): δ =166.68 (C8 and C8′), 162.59 (C13 and C13′), 147.55 (C6) 140.64(C5), 134.84(C2), 134.08(C3), 133.12(C4), 119.80(C9 and C9′), 119.63(C10 and C10′), 119.20(C11 and C11′), 118.25(C12 and C12′), 118.07(C14 and C14′). $C_{19}H_{14}BrN_3O_2$ (calculated mass 396): observed mass $[M + H]^{-}$ =395 [Fig. S2a, S2b & S3].

4. Results and discussion

4.1. Photo physical properties of BAMD molecule

The normalized UV–Vis absorption spectra of BAMD was recorded in phosphate buffer at pH=7.4. The absorption spectra shows two absorbance maxima at 297 and 435 nm corresponding to π-π* and n-π* transitions, respectively (Fig. S4a). Similarly, the fluorescent property of BAMD molecule was studied at 435 nm as excitation wavelength at neutral pH (7.4). The BAMD exhibited a sharp fluorescence peak at 550 nm with very good fluorescence intensity (Fig. S4b). Then, effect of pH on fluorescent property of the BAMD was also studied in different buffer solutions (from pH 2–12.5). When the pH was adjusted from 2 to 6, there was a gradual increment in fluorescent intensity up to pH (7.4). But, on further increase from 7.4 to 12.5, the fluorescent intensity decreased along with blue shift (Fig. S6). The maximum fluorescent intensity was obtained at pH=7.4. Hence, all spectroscopic measurements were carried out in phosphate buffer (pH 7.4). This phenomenon may be due to that at low pHs, BAMD may be existing in protonated form which leads to inhibition of electronic charge transfer among the molecule and results a poor increment in fluorescent intensity. But under neutral medium, the molecule emits very high intensity due to the availability of lone pair electrons of hydroxyl group of BAMD for complete electron delocalization. Meanwhile, in basic medium, deprotonation may lead to the internal charge transfer process among the molecule and it is clearly supported by observing a remarkable blue shift along the decrement in intensity and results in green fluorescent color (Masayasu et al., 2008; Lin et al., 2009; Ellairaja et al., 2015).

The quantum yield of BAMD was calculated using the data obtained from on the UV and Emission under optimized condition, as 0.85 (λ_{ex}=435 nm). In this study, Rhodamine 6 G was used as a standard in

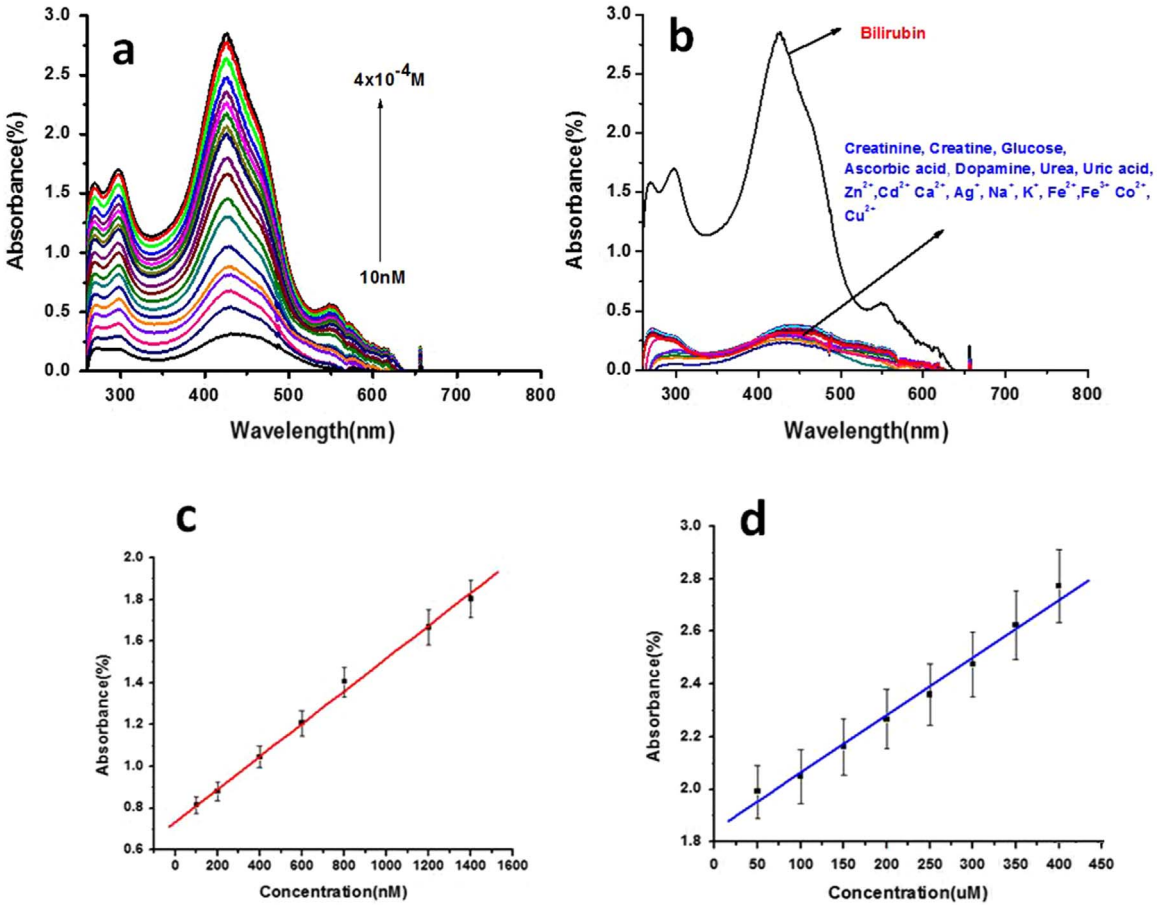

Fig. 1. (a) UV–vis spectra of BAMD while adding varying the concentration of bilirubin from 10 nM to 4×10^{-4} M. (b) Selective recognition of bilirubin by of BAMD in presence of other interfering biomolecules and metal ions. (c) and (d) linear range for the selective detection of bilirubin at nano and micromolar concentration ranges. [Concentrations of BAMD is 5×10^{-5} M, and other biomolecules and metal ions are 4×10^{-4} M, at pH 7.4, Phosphate buffer].

ethanol (λ_{ex}=480 nm, Φ=0.95). The quantum yield of BAMD is comparable with standard Rhodamine 6 G dye. Since, the BAMD possessed high fluorescent intensity as well as quantum yield; it was applied for designing of optical biosensors for detection of bilirubin. [Calculation was given in Supporting information]

4.2. Designing of BAMD based colorimetry biosensor for bilirubin detection

For sensor application, bilirubin was first dissolved in DMSO due to its poor solubility and then further diluted to different concentrations by using phosphate buffer. Then, UV–vis analysis was examined by taking 5×10^{-5} M BAMD in phosphate Buffer (pH 7.4). The different concentrations of bilirubin were added to BAMD solution and incubated for 10 min. The UV–Vis spectra were recorded before and after the addition of bilirubin. While adding different concentrations of bilirubin from 10 nM to 4×10^{-4} M, there was a gradual increment in the absorbance **(**Fig. 1**a).** The selectivity of BAMD towards bilirubin in the presence of higher (1×10^{-3} M) **(**Fig. S5**)** and lower (4×10^{-4} M) **(**Fig. 1**b)** concentrations of interfering biomolecules and metal ions was also checked at both the pHs. From the UV-spectral results, it is clearly understood that the interaction of BAMD with bilirubin is more selective. It is also noted that after the addition of bilirubin into BAMD solution, the initial color of BAMD solution has been changed from slight yellow to light yellowish orange through naked eye. But there was no color change for the addition of interfering biomolecules and biologically important metal ions. It indicates that the biosensor can colorimetrically sense bilirubin selectively.

4.3. Fluorescent response of BAMD towards bilirubin

Under the optimized condition, the synthesized molecule exhibited a sharp fluorescence peak at 550 nm with very good fluorescence intensity **(**Fig. S4b**).** When the bilirubin was added, quenching was observed. Then, the concentration of bilirubin was varied gradually, and steady quenching in fluorescent intensity was observed from 1 pM to 500 μM **(**Fig. 2**a).** The same kind of quenching phenomenon was observed at pH 9.0 also **(**Fig. S8**).** The linear range is found to be 1 pM–500 μM at pH 7.4. LOD is found to be 2.8 pM and 3.3 pM at pH 7.4 **(**Fig. 2**b)** and 9.0, respectively **(**Fig. S11**).** [The calculations were given in Supporting information].

For the very first time, an excellent LOD of 2.8 and 3.3 pM along with wide linear detection range for bilirubin was obtained and compare to the previous electrochemical and optical sensors **(**Table 1**).**

4.4. Selective and competitive recognition of bilirubin amongst biologically interferents

It is well known that human test samples like urine and human serum consist of so many biomolecules. Hence, the interference studies of the biomolecules such as creatine, creatinine, glucose ascorbic acid, L-dopamine, urea, and uric acid and biologically important metal ions like Zn^{2+}, Cd $^{2+}$ Ca^{2+}, Ag^{+}, Na^{+}, K^{+}, Fe^{2+} Fe^{3+}, Co^{2+}, and Cu^{2+}(500 μM) were tested during the determination of bilirubin at higher concentration (500 μM) in pH 7.4 **(**Fig. 3**a)** and 9.0 **(**Fig. 3**b)**. From the data, it is understood that the probe shows high selectivity for bilirubin. Because, except bilirubin, all other interferents did not exhibit absorption and emitting properties, **(**Senthilkumar and Asha, 2015**).** So, this confirms

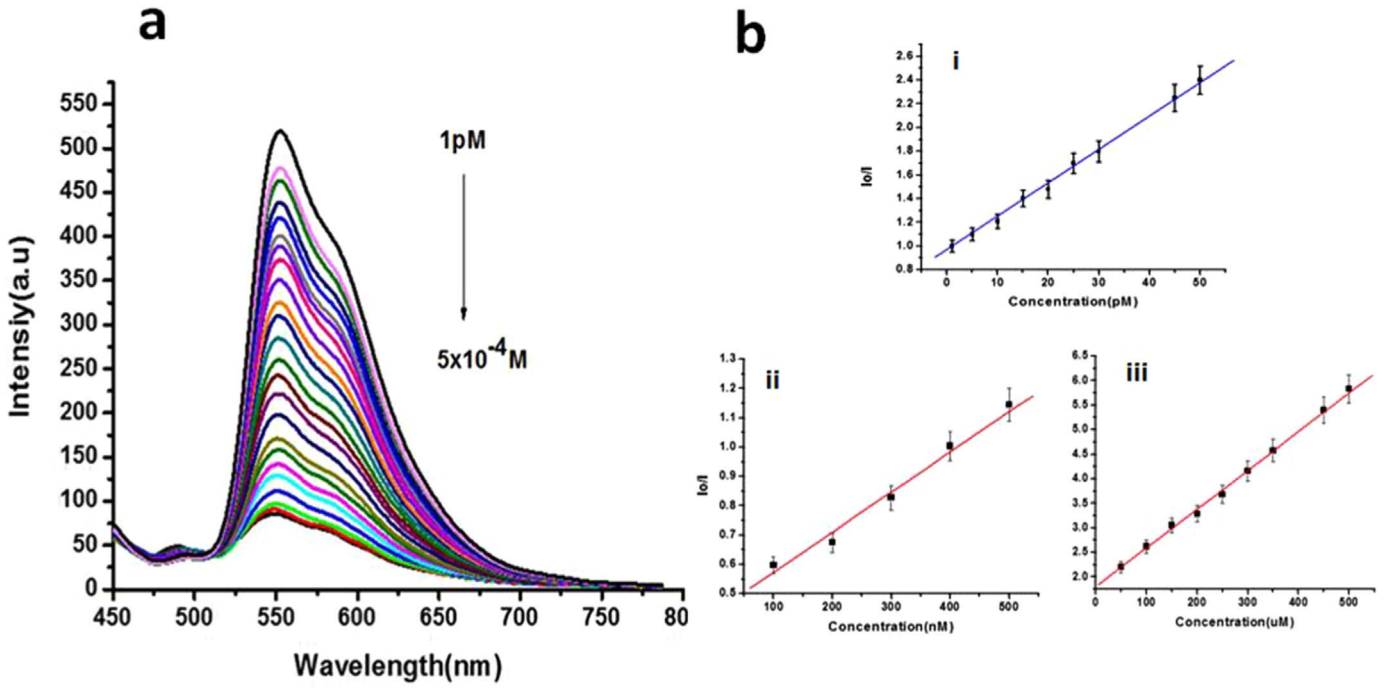

Fig. 2. (a) Emission spectra for the synthesized BAMD while varying the concentration of bilirubin from 1 pM to 500 μM. (b) (i), (ii) and (iii) Linear range for the selective detection of bilirubin at pico, nano and micromolar concentration ranges, respectively. [Concentration of BAMD molecule is 5×10^{-5} M, at pH7.4, Phosphate buffer].

FRET mechanism between bilirubin molecule and probe. Generally, Hydrogen bonding plays a vital role in FRET based fluorescent biosensor. Among other interferents, bilirubin has very good tendency to form intra and inter molecular hydrogen because of its unique structural **(**Hsieh and Morris, 1988**;** Brown et al., 2001**)**. Though competition for binding sites could be expected to be present in the pool of interferences, binding of bilirubin in minimum sites was sufficient for FRET-based energy transfer to occur due to the well-known molecular wire effect **(**Zhou and Swager, 1995**)**.

The competitive recognition studies were also carried out separately in presence of interfering molecules at lower (1 pM) and higher concentrations (500 μM). Briefly, two equivalents (40 μL) of interfering molecules (1×10^{-3} M) were added to the solution containing one equivalent of bilirubin (20 μL) and the corresponding fluorescence spectral changes were recorded. In both concentration ranges, BAMD showed selective sensing towards bilirubin at pH 7.4 **(**Fig. 3**b and d)** as well as **pH 9.0 (**Fig. S9a–d**).** Only a negligible quenching of 3.2% and 5% were observed for creatine and Cu^{2+} ions at higher concentration of bilirubin (500 μM) at pH 7.4. The experiments were also carried out to check the reproducibility **(**Fig. S14**).** The results clearly suggest the developed biosensor is highly reproducible and corresponding related standard deviation (RSD) value is given in supporting information.

5. Fluorescence life time counting study

Lifetime fluorescence studies generally investigate the change in fluorescence phenomenon or decay rate of the fluorescent molecule over time when irradiated with UV–vis, or near-IR light. The life time usually varies based on the fluorescent nature of the compounds. (Lakowicz, 2006). In our current report, the time-correlated single photon counting (TCSPC) analysis was utilized in order to understand the interaction between BAMD and bilirubin. The Time-resolved fluorescence decay was recorded for BAMD at 435 nm with excitation from nano LED at 435 nm and 550 nm in phosphate buffer at pH=7.4 at 25 °C. After the addition of bilirubin, the decay curves of BAMD are fitting into biexponential fit **(**Fig. S12a**,** Table S1**)**. The details of lifetime study are given in supporting information. BAMD exhibited lifetime of τ1=870 ps and τ2=1.7 ns with B1=0.0517 and B2=0.038. Upon the addition of various concentrations of bilirubin, the lifetime of the probe molecule decreased to a minimum value of τ1=100 ps and τ2=2.0 ns with B1=0.067 and α2=0.019. Hence, BAMD shows a very good life time (τ) when compare to the previous report (Senthilkumar and Asha, 2015). The lifetime is also measured at pH 9.0 and all those

Table 1
Comparative performance of this BAMD based biosensor with previously reported bilirubin biosensors.

Sl. No.	Types of sensors for bilirubin reported	LOD	Linear range	Reference
1.	Non-Enzymatic Graphene/Polystyrene-Electrochemical method	2 μM	0–450 μM	Nolan and Lippard, 2007
2.	BoX/Gold/nanorods-Electrochemical method	0.005 μM	0.01–100 μM	Yoon et al., 2005
3.	BoX-MWCNT-Amperometric array based method	8 μM	0–150 μM	Vidal et al., 1999
4.	Box-Polytetrathiophene –Mn (II) complex-Amperometric Method	40 μM	0.1–50 μM	Taurino et al., 2012
5.	BoX-Oxygen electrode- Electrochemical method	10 μM	10–200 μM	Jana et al., 2001
6.	Ferrocene caboxamide/MWCNT/AuNPS	1.2 μM	1.2–100 μM	Chen et al., 2005
7.	Surfactant based Fluorimetric method	0.007 μM	0.1–17 μM	Aiken and Huie, 1991
8.	HSA-Gold nanoclusters- Fluorimetric method	248 nM	0.5–7 μM	Ellen and Timothy, 2003
9.	Polyfluorene polymer- D-Glucuronic acid-Fluorimetric method	150 nM	25–50 μM	Ravi et al., 2015
10.	**BAMD- fluoresecent molecule based biosensor**	**2.8 pM(pH=7.4) 3.3 pM(pH=9.0)**	**1 pM–500 μM**	**Present work**

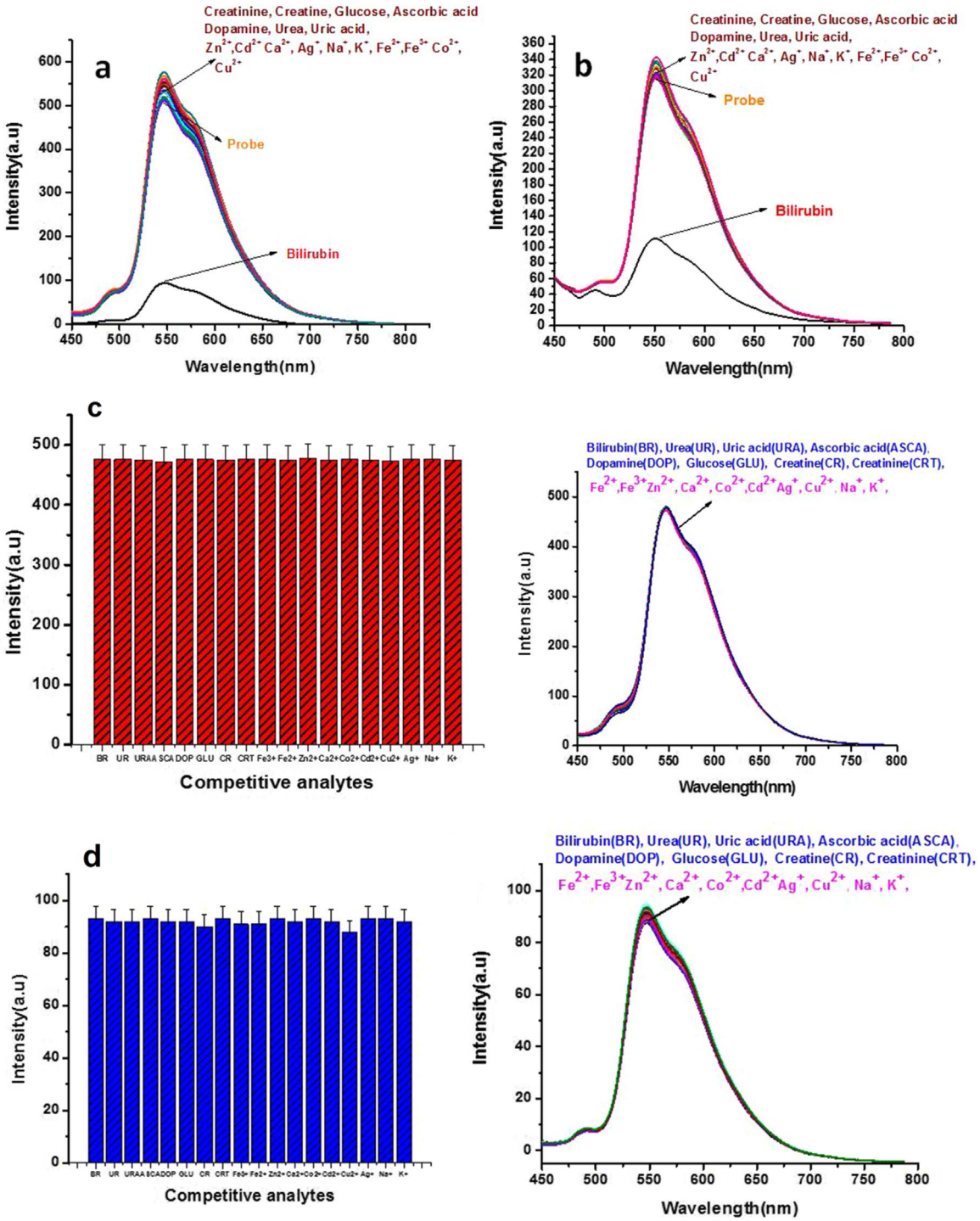

Fig. 3. (a) and (b) Emission spectra of BAMD for selective detection of bilirubin in presence of interfering biomolecules and metal ions at pH=7.4 [Phosphate buffer] and pH=9.0 [ammonium buffer] respectively. (c) Bar diagram (Left) for competitive studies using BAMD molecule along with 1equivalent (10 μL) of bilirubin at lower [1 pM] and (d) higher concentration [500 μM] in the presence of 2 equivalents (20 μL) of other biomolecules, metal ions (μM) along with corresponding emission spectra (Right) [Concentration of BAMD is 5×10^{-5} M and bilirubin and other interferents were maintained at 5×10^{-4} M for selectivity studies and 1×10^{-3} M for competitive analysis in respective buffers].

details are given in supporting Information **[**Fig. S12b**,** Table S2**]**.

6. Sensing of bilirubin in human serum

The biological application of the biosensor is demonstrated by the quantitative estimation of bilirubin in human blood and urine sample. **[**Fig. 4 **(a, b and c)]** The unknown concentrations of bilirubin were determined by the standard addition method. Briefly, some known concentrations (30 and 50 pM, 300 and 500 nM, 100–500 μM) of bilirubin was spiked with test samples like human serum and urine. The results obtained are compared with the previous emission data using bilirubin as analyte. From the results, it is clearly understood that the developed biosensor can be used for the detection of bilirubin in human serum and urine. **(**Table S3, S4 & S5**)**.

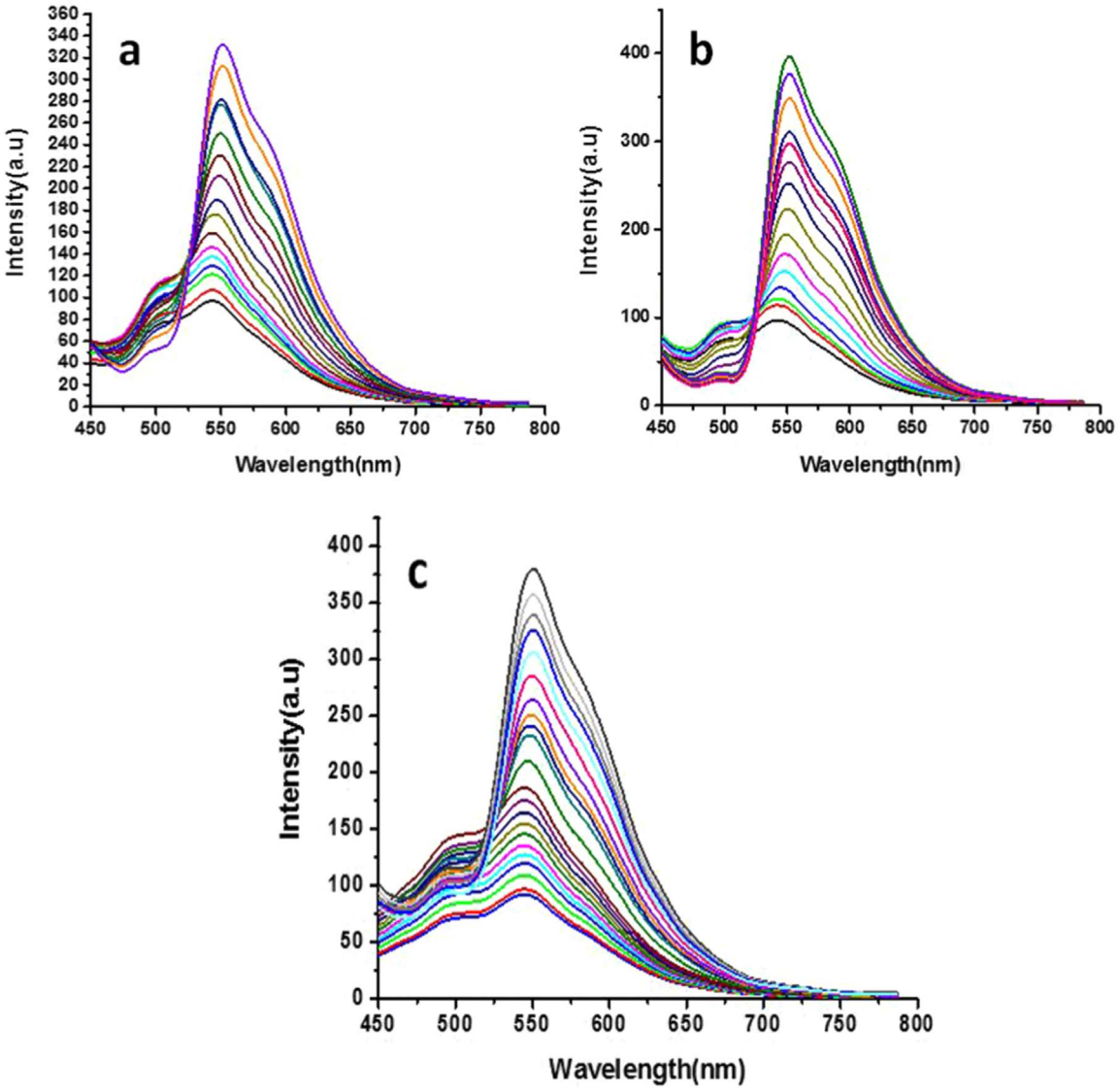

Fig. 4. Selective emission Spectra for the determination of bilirubin in human serum (a and b) obtained from two persons 1 and 2, human urine sample (c) obtained from person 3. [Concentration of bilirubin spiked: 30 and 50 pM, 300 and 500 nM, 100–500 μM].

7. Bilirubin sensing mechanism FRET based on fluorescence analysis

In general, the FRET mechanism is confirmed by analyzing the spectral overlaps of both UV and Emission data **(**Scheme 1**b),** the quenching fluorescent intensity and life time of the probe. Based on the spectral overlapping of UV and emission profiles, it is understand that the interaction between BAMD and bilirubin adopted FRET mechanism in the stoichiometry of 1:2. **(Job's plot,** Fig. S10**).** This mechanism is further supported and confirmed by the Stern-Volmer quenching constant and quenching efficiency were calculated based from the linear graph between bilirubin variation and fluorescence intensity of the probe **(**Fig. 2**b).** [Details were given in Supporting information].

Very good quenching efficiencies of 83.62% and 65.16% were attained, when the bilirubin concentration was increased up to 500 μM and 250 μM at pH 7.4 and 9.0, respectively. The K_{SV} was calculated to be $3.3\times10^{10}\ M^{-1}$ and $7.6\times10^{9}\ M^{-1}$ at pH 7.4, pH 9.0 respectively. This large quenching constant has suggested that the bilirubin is a very good acceptor for BAMD donor molecule. Generally, besides FRET, the fluorescence quenching of fluorophores by analytes can also be dominated by the mechanism of electron transfer or inner filter effect (IFE). However, no obvious red or blue shift of the fluorescence emission spectra was observed when interacting with bilirubin **(**Fig. 2**a).** So, all the above results are strongly supporting FRET mechanism occurring during the interaction between BAMD and bilirubin **(**Scheme 1**a).**

8. Naked eye and UV-lamp detection of bilirubin

At neutral medium (pH=7.4), the initial color of BAMD changed from colorless to yellow which increasing the concentration of bilirubin. But in basic pH (9.0), the slight yellow color of BAMD changed to orange color. **(**Fig. S13a**)** Whereas in fluorescence analysis, at pH 7.4 the initial slight yellow color fluorescent of BAMD changed to orange color. Interestingly, the increasing the concentration of bilirubin just enhances the intensity of the color. In basic medium, the initial slight yellow color of BAMD changed to green fluorescence (deprotonated form) while varying the concentration of bilirubin. **(**Fig. S13b**)**. Both the naked eye and UV lamp color change tests prominently show the applicability of developed sensor for the bilirubin detection.

9. Conclusion

A green and facile imine based fluorescent molecule, BAMD, was

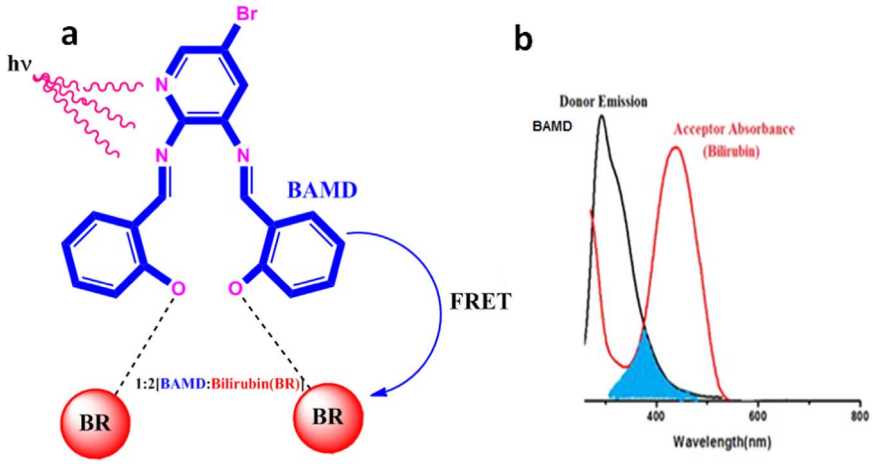

Scheme 1. (a) A tentative schematic representation of the proposed FRET mechanism which could occurred between the donor (BAMD) and acceptor (Bilirubin) molecule. (b) Overlapping of absorbance spectra of Acceptor (Bilirubin) and emission spectra of Donor (BAMD) to support the FRET Mechanism. **Quenching Constant at pH 7.4. Io/I =3.3C_{BR}+1(R^2=0.9987). Quenching Constant at pH 9.0. Io/I =7.6C_{BR}+1(R^2=0.9985)**.

synthesized through green methodology and characterized by NMR and ESI mass techniques. Using BAMD, highly selective and sensitive biosensor was developed for bilirubin at pH 7.4 and 9.0. The limit of detections are found to be 2.8 pM and 3.3 pM at pH=7.4 and pH=9, respectively within the linear range of bilirubin concentration from 1 pM–500 μM. BAMD shows a very good quantum yield of 0.85 along with an excellent life time of 870 ps at pH=7.4. Further, the biosensor was applied for the detection of direct bilirubin in both human blood and urine samples through standard addition method. A very good recovery was obtained towards bilirubin.

Acknowledgement

This work is financially supported by DST-INSPIRE Fellowship Scheme, New Delhi, India (grant no. DST/INSPIRE-Fellowship/2012/251). So, the author thanks DST for offering the fellowship for pursuing his Ph.D program. Finally, the author specially thanks Dr. S. Eswaramoorthy, Scientist; CLRI has providing the Life time instrument facility.

Appendix A. Supporting information

Supplementary data associated with this article can be found in the online version at doi:10.1016/j.bios.2016.12.026.

References

Aiken, J.H., Huie, C.W., 1991. Anal. Lett. 24, 167–180.
Ambler, J.A., 1929. Ind. Eng. Chem. 21 (1), 47–50.
Ameri, M., Schnaars, H., Sibley, J., Honor, D., 2011. J. Vet. Diagn. Invest. 23 (1), 120–123.
Anjali, J., Shabana, Y., Kumar, D.N., 2013. ***Int*** J. Pharm. Bio Sci. 4 (4), 197–204.
Atsushi, I., Asuka, F., Takeshi, W., Takayuki, E., Naohiko, M., 1996. J. Phys. Chem. 100, 16053–16057.
Balamurugan, T., Sheela, B., 2015. RSC Adv. 5, 50470–50477.
Batra, B., Lata, S., Sunny, Rana, J.S., Pundir, C.S., 2013. Biosens. Bioelectron. 44, 64–69.
Brown, S.P., Zhu, X.X., Saalwachter, K., Spiess, H.W., 2001. J. Am. Chem. Soc. 123, 4275–4285.
Cheifetz, A.S., Brown, A., Curry, M., Moss, A.C., 2010. Oxford American Handbook of Gastroenterology and HepatologyUSA. Oxford University Press, Oxford, 165, (ISBN 0199830126).
Chen, H.M., Peng, H.C., Liu, R.S., Asakura, K., Lee, C.L., Lee, J.F., Hu, S.F., 2005. J. Phy. Chem. B. 109, 19553–19555.
Christabel, T.T., Cheng-Wei, T.C., 2009. J. Org. Chem. 74, 634–644.
Cintas, P., Luche, J.L., 1999. Green. Chem. 1, 115–125.
Cravotto, G., Cintas, P., 2006. Chem. Soc. Rev. 35, 180–196.
Cuihua, X., Venkat, R.R.D., Haiying, L., 2006. Macromolecules 39, 5747–5752.
De Silva, A.P., Gunaratne, H.Q., Gunnlaugsson, T., Huxley, A.J.M., McCoy, C.P., Rademacher, J.T., Rice, T.E., 1997. Chem. Rev. 97, 1515–1566.
Ellairaja, S., Manikandan, R., Vijayan, M.T., Rajagopal, S., Vasantha, V.S., 2015. RSC Adv. 5, 63287–63295.
Ellen, K.F., Timothy, E.G., 2003. J. Am. Chem. Soc. 125, 16174–16175.
Feng, Q., Du, Y., Zhang, C., Zheng, Z., Hu, F., Wang, Z., Wang, C., 2013. Sens. Actuators B. 185, 337–344.
Gary, K., Ronald, M.S., 1980. J. Phys. Chem. 84, 2262–2265.
Jagriti, N., Nidhi, C., Ashish, M., Vivek, C., Pundir, C.S., 2015. Adv. Mater. Lett. 6 (11), 1012–1017.
Jana, N.R., Gearheart, L., Murphy, C., 2001. J. Adv. Mater. 13, 1389–1393.
Kannan, P., Chen, H., Lee, V.T.W., Kim, D.H., 2011. Talanta 86, 400–407.
Komatsu, K., Urano, Y., Kojima, H., Nagano, T., 2007. J. Am. Chem. Soc. 129, 13447–13454.
Kwon, J.Y., Jang, Y.J., Lee, Y.J., Kim, K.M., Seo, M.S., Nam, W., Yoon, J.A., 2005. J. Am. Chem. Soc. 127, 10107–10111.
Lakowicz, J.R., 2006. Principles of Fluorescence Spectroscopy 3rd ed.. Springer, (ISBN 978-0387-31278).
Leo, F., Kline, O.L., 1950. J. Biol. Chem. 184, 599–606.
Lin, X., Chun, L., Hua, J., 2009. Org. Lett. 11, 1655–1658.
Masayasu, T., Mika, Desaki, Akio, Ojida, Shohei, Iyoshi, Tasuku, Hirayama, Itaru, Hamachi, Yukio, Yamamoto, 2008. J. Am. Chem. Soc. 130, 12564–12565.
Hsieh, Y.Z., Morris, M.D., 1988. J. Am. Chem. Soc. 110, 63–66.
Mason, T.J., 1997. Chem. Soc. Rev. 26, 443–451.
Miao, X., Li, Z., Ling, L., 2016. Analyst 141, 5829–5834.
Morimoto, Y., Ishihara, T., Takayama, M., Kaito, M., Adachi, Y., 2000. J. Clin. Lab. Anal. 14 (1), 27–31.
Nolan, E.M., Lippard, S.J., 2007. J. Am. Chem. Soc. 129, 5910–5918.
Oscar, R.M., Xiaoning, Li, Limary, G.G., Zheng-Jiang, Z., Bo, Y., Uwe, H.F.B., Vincent, M.R., 2011. J. Am. Chem. Soc. 133, 9650–9653.
Rand, R.N., di Pasqua, A., 1962. Clin. Chem. 8, 570–578.
Ravi, S.L., Matthew, S.M., Hien, M.N., 2015. Biomacromolecules 16, 4013–4021.
Reem, M.A., Moustafa, M.H., 2010. Arab. J. Chem. 3, 257–264.
Santhosh, M., Chinnadayyala, S.R., Kakoti, A., Goswami, P., 2014. Biosens. Bioelectron. 59, 370–376.
Senthilkumar, T., Asha, S.K., 2015. Macromolecules 48 (11), 3449–3461.
Silbernagl, S., Despopoulos, A., 2009. Color Atlas of Physiology 6th ed.. Thieme, Stuttgart, 252.
Soojin, K., Jin, Y.N., Young, K., Jin, H.K., Hee, K., Seong, W.N., So, H.K., Sungsu, P., Cheal, K., Jinheung, K., 2012. Inorg. Chem. 51, 3597–3602.
Taurino, I., Micheli, G., De Carrara, S.,, 2012. BioNanoScience 2, 185–195.
Thomas, A.B., Tupe, P.N., Badhe, R.V., Nanda, R.K., Kothapalli, L.P., Paradkar, O.D., Sharma, P.A., Deshpande, A.D., 2009. Green. Chem. Lett. Rev. 2, 23–27.
Thor, W., Ruud, H., 2010. NeoReviews ISSUE 6, 11.
Vidal, M.M., Gil, M.H., Delgadillo, I., Alonso, J., 1999. J. Biomater. 20 (8), 757–763.
Wang, J., Qian, X., Cui, J., 2006. J. Org. Chem. 71, 4308–4311.
Xiao, Z., Guo, X., Ling, L., 2013. Chem. Commun. 49, 3573–3575.
Yoon, S., Albers, A.E., Wong, A.P., Chang, C.J., 2005. J. Am. Chem. Soc. 127, 16030–16031.
Zhou, Q., Swager, T.M., 1995. J. Am. Chem. Soc. 117, 7017–7018.